CONVERTING COFFEE SILVERSKIN TO VALUE-ADDED PRODUCTS BY A SLOW PYROLYSIS-BASED BIOREFINERY PROCESS

Cristina del Pozo[1*], Filipe Rego[3], Yang Yang[3*], Neus Puy[1,2], Jordi Bartrolí[1], Esteve Fàbregas[1], Anthony V. Bridgwater[3]

[1] *Department of Chemistry, Universitat Autònoma de Barcelona (UAB), Edifici Cn, Campus de la UAB, 08193 Cerdanyola del Vallès, Barcelona, Spain.*

[2] *Forest Science and Technology Centre of Catalonia (CTFC). Crta. Sant Llorenç de Morunys, km 2. 25280 Solsona, Lleida, Spain.*

[3] *Bioenergy Research Group, EBRI, Aston University, Birmingham B4 7ET, United Kingdom*

* Corresponding author: Cristina.DelPozo@uab.cat / crisdelpozo19@gmail.com (C. del Pozo); y.yang6@aston.ac.uk (Y.Yang)

Abstract

This work aims to transform coffee silverskin (CSS), the only waste from the coffee roasting process, that worldwide amounts to about 76 million kg/year, into value-added products within an integrated slow pyrolysis process. The study, performed at 280 °C, 400 °C and 500 °C, determined the potential applications of the resulting fractions. Biochar has been studied as an adsorbent of organic pollutants in water, using methylene blue (MB) and methyl orange (MO), which are respectively cationic and anionic aromatic dyes, as model compounds, and with 400 ºC biochar giving the highest removal values, at 98% with MB and 40% with MO. Moreover, CSS biochar could be used to obtain renewable energy from its combustion, with 22.6 - 24.2 MJ/kg calorific values. The liquid fraction could be a potential source of caffeine,

among phenolics, with 400 ºC aqueous phase presenting the highest concentration of caffeine (14.3 g/L). Concerning the gas fraction, it could be used to obtain heat for biomass drying before pyrolysis. Hence, use of the pyrolysis products as described would allow zero-waste to be achieved in the coffee roasting industry, thus promoting the green and circular economy and production of green chemicals and materials in a biorefinery context.

Keywords

Coffee silverskin; slow pyrolysis; pyrolysis liquid; biochar; adsorption; caffeine

1. Introduction

Coffee is one of the most commonly consumed beverages worldwide [1]. The roasted coffee beans are produced in the coffee consuming countries from the roasting process of green coffee beans [2], which are cultivated and imported from tropical areas. Specifically, the most coffee consuming regions are EU, USA and Brazil, with around 2.8, 1.6 and 1.3 billion kg consumed in 2018/19 season respectively. From the roasting process, it is obtained 84% wt. of roasted coffee and around 0.75% wt. of coffee silverskin (CSS), which is the protective skin of beans that shed during the process [1,3]. CSS is the only by-product from the coffee roasting process, but it is generated on a large scale [4], amounting to about 76 million kg per year since at least 2016 [1,5]. CSS is composed by a high amount of dietary fibre (56–62%); it contains cellulose (18%), hemicellulose (13%) and it is also rich in protein (19%) and minerals (8% ash) [6]. Nowadays, most CSS is discarded and often used as firelighters or dispatched to landfills [1,7], representing a serious environmental problem due to the phytotoxicity of this waste as a result of its high content of caffeine, polyphenols, and tannins [8]. Therefore, it is necessary to look for greener waste management alternatives, by

converting the residue to a resource and complying with green solutions and circular economy (zero waste approach).

Pyrolysis is a widely used treatment to transform biomass into value-added products. This treatment, performed at elevated temperatures in the absence (or limited concentration) of oxygen, decomposes the main polymers of biomass (hemicellulose, cellulose and lignin) into liquid, gas and solid fractions [9]. The pyrolysis liquid and gas fractions could be used as chemical and energy sources respectively, whereas the solid fraction (biochar) could be considered as a value-added product itself due to the broad range of applications it has. Hence, this work uses pyrolysis to completely valorise CSS, aiming to reach zero-waste in the coffee roasting industry. Specifically, the treatment performed was slow pyrolysis in a lab-scale reactor with a capacity of 0.3 kg/h at 280 °C, 400 °C and 500 °C, with temperature being one of the main factors influencing the properties and proportion of the products. However, and to the best of our knowledge, only a few papers have been addressed on the pyrolysis of CSS and the valorisation of the resulting products. Polidoro et al. [8] optimised the pyrolysis process (slow pyrolysis) focusing on the pyrolysis liquid yield and its use as source of chemicals. On the other hand, a previous study from our research group [10] regarded the valorisation of CSS by slow pyrolysis in a pilot plant with a capacity of 15 kg/h, based mainly on pyrolysis liquid as a source of phenolics, and biochar as a solid fuel. There is not yet a detailed study of all CSS pyrolysis products, information that would allow to determine their potential applications.

In this sense, biochar has been attracting increasing attention due to its versatility and environmental benefits [11], with large number of studies highlighting its use in terms of mitigating global warming by means of carbon sequestration [12], and as a soil amendment to enhance crop yields [13–15]. Several studies also reported that biochar showed excellent ability to remove contaminants such as heavy metals and organic pollutants from water

Formatted: Font color: Text 1

Formatted: Font color: Text 1

Formatted: Font color: Text 1

Formatted: Font color: Text 1

Formatted: Font color: Text 1

[13,15,16], since it can present large specific surface area, porous structure, abundant surface functional groups and mineral components, which suggests its use as a contaminant adsorbent [11,15,17]. The continuous development of industry and agriculture in recent years has increased the level of pollutants in the environment, seriously threatening ecology and human health [11,18]. Of the many ways to remove dissolved water contaminants, adsorption is widely considered to be superior to other processing technologies in terms of cost, viability and effectiveness [11,19,20]. Hence, the role of biochar as an adsorbent has gained attention mainly due to its low-cost, high-efficiency and renewable characteristics [11]. A large number of researchers also showed that biochar can have good adsorption of polycyclic aromatic hydrocarbons [21], herbicides [22], pesticides [17], antibiotics [23] and dyes [24], recently becoming a research hotspot in the environmental science field [11].

Based on the above, this work has studied the properties of CSS biochar as an adsorbent of organic pollutants in aqueous media. The study has been carried out using methylene blue (MB) and methyl orange (MO) as model compounds [25] in order to assess the adsorption performance of CSS biochar. MB and MO are respectively cationic and anionic aromatic dyes that may present same adsorption mechanisms on CSS biochar as other contaminants with similar structures. Some of these mechanisms can include electrostatic and aromatic π–π interactions, hydrogen bonds, and pore-filling [13]. Apart from their function as model adsorbates, MB and MO are also extensively used in fabric staining [20,26]. With the rapid development of the textile industry, dye effluents account for a large proportion of industrial wastewater, and have become a significant source of pollution [11], organic dyes being well known as toxic and carcinogenic substances [20]. Hence, the evaluation of the removal efficiency of MB and MO by CSS biochar is in itself of great interest. The use of CSS biochar as an adsorbent could protect the environment by both removing pollutants from water and improving the waste management of CSS. In order to increase the efficiency of

Formatted: Font color: Text 1

Formatted: Font color: Text 1

Formatted: Font color: Text 1

biochars as adsorbents, they are usually activated with KOH, steam or carbon dioxide, increasing its surface area and functional groups. The activation process can ~~be~~ however be prohibitively expensive at a large scale [16], so in this work, the study has been performed with the original biochar as ~~it was~~ produced.

Regarding CSS pyrolysis liquid, it has been described as a source of phenolics and caffeine, among other value-added compounds [8,10]. Phenolics, which have been quantified in our previous study by Folin-Ciocalteu and DPPH methods [10], are highly valuated in nutraceuticals and cosmetic industries [9,10] due to their antioxidant properties. Caffeine, on the other hand, presents stimulant effects on the nervous, muscular and cardiovascular systems, being used in a wide array of beverages and pharmaceutical products [27–29], and so, making its quantification interesting. Hence, CSS pyrolysis liquid could be studied as a potential source of value-added compounds, which may differ from the previous work [10] due to the reactor used in that case (pilot plant) was different from the one used in the present study (lab-scale reactor).

With~~In~~ reference to the gas fraction, it can be composed of CO, H_2 and CH_4, which are combustible gases, and so, a potential energy source [12].

The objective of the present work is to study and characterise the solid, liquid and gas products resulting from the slow pyrolysis of CSS in a lab-scale reactor at 280 °C, 400 °C and 500 °C, in order to determine the potential applications of each pyrolysis fraction within an integrated CSS biorefinery context. In this way, and for the first time, biochar from CSS has been studied as an absorbent of organic pollutants in aqueous media; CSS pyrolysis liquids have been considered as a source for caffeine production with quantitative analysis; and the gas fraction has been valuated as an energy source. The valorisation of the CSS pyrolysis products would allow to achieve zero-waste in the coffee roasting industry and contribute to circular economy and bioeconomy, promoting the production of green

Formatted: Font color: Text 1
Formatted: Font color: Text 1
Formatted: Font color: Text 1
Formatted: Font color: Text 1
Formatted: Font color: Text 1
Formatted: Font color: Text 1
Field Code Changed
Formatted: Font color: Text 1
Formatted: Font color: Text 1
Formatted: Font color: Text 1
Formatted: Font color: Text 1
Formatted: Font color: Text 1
Formatted: Font color: Text 1
Formatted: Font color: Text 1

chemicals and materials and representing a potential improvement for the economy and the environment.

2. Materials and methods

2.1. Feedstock

CSS was supplied by a roasting coffee company from Spain in briquette format. The CSS briquette was crushed and sieved to a homogeneous particle size of 1 mm, before pyrolysis. The moisture of CSS (1 mm) was 10.1 wt. % (data obtained from the loss of weight from heating 1.5 g of CSS at 105 ºC overnight; 0.15 of standard deviation; measurement performed in triplicate and averaged).

2.2 Reactor system

Slow pyrolysis of CSS was performed at 280 °C, 400 °C and 500 °C in a bench-scale auger reactor described elsewhere [30]. Nitrogen gas was used to purge and remove oxygen from the system. The solid residence time was fixed at 10 min and the feeding rate at 300 g/h. The solid product was collected from the char collection vessel, after cooling to room temperature, and placed in a sealed plastic bag for further physicochemical analysis. The condensable vapours were collected from a cooling and liquid collection system, comprised of a water-cooled condenser fixed at 20 ºC (flask 1) and two ice-fingers filled with dry ice and acetone (flasks 2 and 3), placed in sealed brown glass containers and stored at 4 °C for further analysis. The non-condensable gases were filtered using a cotton filter, passed through a gas meter and analysed every 3 min by an online MicroGC in order to analyse the gas distribution (GC; VARIAN CP-4900, USA).

2.3 Product yields

Yields of solid, liquid and gas fractions, from each pyrolysis experiment, were calculated by dividing the mass of the resulting pyrolysis products by the mass of the feedstock used in the experiment. Data was expressed as wt. % on dry feedstock basis.

Biochar was weighed after cooling and collected from the char collection vessel. Liquid product weight was obtained from the difference between the mass of the glassware for liquid collection after the pyrolysis experiment and before. The 280 ºC pyrolysis liquid only presented one phase. Two-phase pyrolysis liquid was obtained from the 400 ºC and 500 ºC pyrolysis experiments; these two phases were separated by decantation and weighed. The weight of gas product was obtained from the volume of the gas, measured by the gas meter, and its density (ρ), calculated from the MicroGC data according to Eq. 1.

$$\rho_{gas} = \sum \frac{\%\,vol_i \cdot \rho_i}{100} \qquad (1)$$

where $\%vol_i$ was the volume percentage obtained from the MicroGC, and ρ_i was the density, of each pyrolysis gas product. Losses of the pyrolysis experiment were calculated by difference.

2.4 Analysis of feedstock and biochars

2.4.1 Feedstock and biochars characterisation

The bulk density of CSS and biochar was measured by weighing 5 mL of sample using a graduated cylinder. The measurement was performed in triplicate.

The ash content was determined following ASTM standards E1755 and D1762 (for biomass and char, respectively), where about 0.5 g of dried sample (105 ºC, overnight) was heated for 30 min at 250 ºC, and then for 6 hours at 750 ºC for biochars and 575 ºC for feedstock. The measurement was performed in triplicate and the results were expressed as wt. % on dry basis.

For subsequent analysis (pH, TGA, FTIR, porosimetry, elemental), CSS and biochars were ground with a mortar and pestle and then sieved to a particle size under 425 μm using a mesh sieve. Before the analyses, the samples were dried at 105 ºC, overnight.

The pH of CSS and biochars was determined in 1:100 wt. sample / distillate water suspension using a pH meter (Sartorius PB-11). The suspension was stirred overnight at 600 rpm before measurement. pH analysis was performed 5 times for each sample and the results averaged.

Thermogravimetric analysis (TGA) of feedstock and biochars was carried out with a Perkin Elmer Pyris 1 TGA, with each sample analysed in duplicate. The analysis was performed by heating the sample from 60 ºC to 900 ºC with a heating rate of 10 °C /min.

Proximate analyses (ash and volatile matter contents) were performed in accordance with the ASTM standards D1762-84 and E1131. The fixed carbon content was calculated by difference.

Surface functional groups of CSS and biochars were characterised by Fourier-transform infrared spectroscopy (FTIR, PIKE Technologies GladiATR and Spectrum software). The scanned wavelengths were 4000 to 400 cm^{-1}, with a resolution of 4 cm^{-1} and using 16 scans. The measurement was performed in duplicate.

Nitrogen porosimetry was measured with a Quantasorb Nova 4000e. The analysis was performed only for the 400 ºC and 500 ºC biochars due to biochars produced at low temperatures are expected to have low surface areas [31]. The samples, weighing between 0.20 and 0.35 g, were outgassed under vacuum at 200 ºC overnight and then, placed into the evacuated sample chamber of the analyser. BET surface area and pore size distribution output was obtained through the Novawin 11.0 software.

Elemental composition (CHNS) of CSS and biochars was determined in duplicate using a Thermo Fisher Scientific Flash 2000 Organic Elemental Analyzer. Oxygen content (on dry basis) was calculated by difference.

Higher Heating Value (HHV) was calculated by the following formula from Channiwala and Parikh [32]:

$$HHV = 0.3491C + 1.1783H + 0.1005S - 0.1034O - 0.0151N - 0.0211Ash \quad \text{(MJ/kg)} \quad (2)$$

C, H, O, N, S and Ash were expressed in mass percentage on dry basis.

2.4.2 Adsorption tests

Methylene blue (MB) (≥82%) and methyl orange (MO) (≥85%), supplied by Sigma-Aldrich, were the dyes chosen to perform the adsorption tests. These tests were conducted in batch, equally for MB and MO, using 25 mg of adsorbent (CSS and biochars, with a particle size under 425 μm) and 10 mL of dye solution (100 mg/L) in a centrifuge tube. The mixture was placed in a sonicator for 3 hours at 50 ºC, and then, it was centrifuged at 3000 rpm for 2 hours. The concentration of dye in the solution was analysed in triplicate using UV- Vis spectrophotometer (Thermo Scientific Evolution 220), on the basis of a linear calibration curve (20-100 mg/L). The results, expressed as percentage of dye removal (%R), were calculated by the following formula [19]:

$$\%R = \frac{100(C_0 - C_t)}{C_0} \quad (3)$$

C_0 (mg/L) was the initial concentration of dye (100 mg/L), and C_t (mg/L) was the concentration of dye after centrifugation step. In order to avoid deviations to the Beer-Lambert Law due to high values (> 2) of absorbance, mixtures were diluted 1:10 with distillate water. The measurements were performed by scanning from 800 nm to 600 nm in the case of MB (maximum wavelength around 670 nm) [19], and from 550 to 350 nm for MO (maximum wavelength of 464 nm) [20].

2.5 Analysis of pyrolysis liquid

Formatted: None

CSS pyrolysis liquid was chemically characterised by gas chromatography – mass spectroscopy (GC-MS). The analysed samples were the ones collected in the first flask, after the water-cooled condenser (see Section 2.2). The analysis was carried out in a Shimadzu GCMS QP2010 SE system equipped with a capillary (Rtx-5MS) column (30 m × 0.25 mm inner diameter × 0.25 μm film thickness). Before injection, samples were diluted in HPLC grade acetone (≧ 99.9%, purchased from Sigma Aldrich), and then filtered (0.45 μg Millipore filter) to avoid obstruction of liner due to suspended ashes/solids after pyrolysis process. A volume of 1 μL was then injected, applying split mode, with the injection port at 300 °C. Helium was used as carrier gas with a flow of 2 mL/min. The oven temperature was as follows: 55 °C for 9 min, 20 °C/ min to 125 °C, 5 °C/min to 325 °C and 325 °C for 10 min. The total run time was 64.50 min. Compounds were identified from the chromatograms by computer matching of mass spectra of the peaks with the National Institute of Standards and Technology (NIST) library; the semi-quantification was performed relating the total area of the compounds, as shown in previous publications [9,10,33].

Caffeine from CSS pyrolysis liquids (aqueous fraction) was quantified by high-performance liquid chromatography system coupled to an ultraviolet-visible detector (HPLC-UV/Vis) (Series 1100, Agilent Technologies). The HPLC-UV/Vis was equipped with a binary pump, a DAD detector and ZORBAX SB-C18 analytical column (4.6 × 100 mm, 1.8 μm particle size) from Agilent Technologies. Water: methanol (60:40, v/v) was used as mobile phase, at a flow rate of 0.4 mL/min at room temperature (25 ºC). 4 μL of sample was injected and caffeine was determinate at the wavelength of maximum absorbance (λ = 273 nm), using an external standard calibration curve with a concentration range of 100 – 1000 ppm. Caffeine content was expressed as g caffeine/L of aqueous phase from the pyrolysis liquid.

2.6 Analysis of gas fraction

Formatted: Font color: Text 1

Formatted: Font color: Text 1

Formatted: Font color: Text 1

Data collected from the MicroGC was processed by the software provided by the manufacturer of the online gas chromatograph (GC; VARIAN CP-4900, USA). The MicroGC used 5Å Molsieve and PortalPLOT columns, and Helium as carrier gas. The chemical composition of gas was obtained by the average of the data corresponding to the pyrolysis process and expressed as % vol.

The heating value of gas was calculated using the following formula [30]:

$$HHV_{gas} = \sum(\%\ vol_i/100) \cdot\ HHV_i \quad (MJ/m^3)\ (4)$$

where % vol_i and HHV_i were the volume percentage and the heating value, respectively, for each gas species present in the pyrolysis gaseous product.

3. Results and discussion

3.1. Slow pyrolysis

3.1.1 Thermal degradation of CSS and biochars

TGA of CSS and biochars resulting from the slow pyrolysis of CSS at 280 °C, 400 °C and 500 °C were carried out in order to study the thermal degradation of CSS during the pyrolysis process. TGA, performed under nitrogen atmosphere, gave information on how the different polymers of biomass (hemicellulose, cellulose, and lignin) degrade in function of the temperature (see Fig. 1).

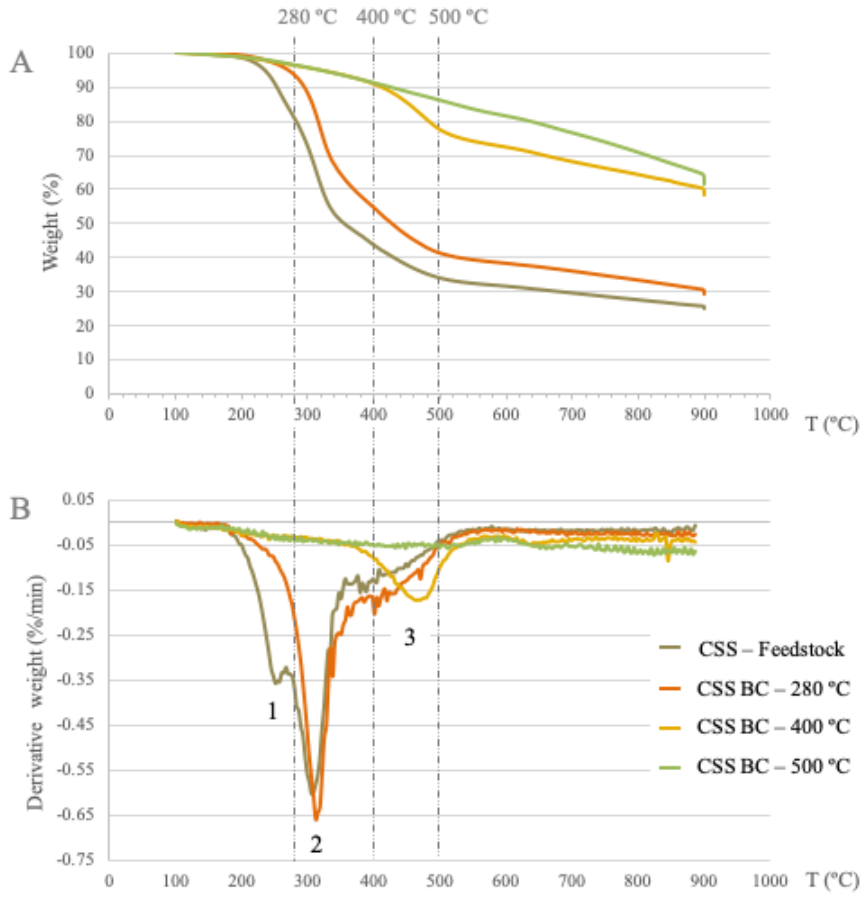

Fig. 1. Pyrolysis curves of CSS and biochars from the slow pyrolysis of CSS, at 280 °C, 400 °C and 500 °C. Graph A shows the weight loss, and graphic B, the rate of weight loss, on dry basis. The numbers correspond to the weight loss mainly associated to hemicellulose (1), cellulose (2) and lignin (3) decomposition. (CSS, coffee silverskin; BC, biochar; T, temperature)

CSS TGA showed two main losses of weight around 255 ºC (1) and 300 ºC (2), attributed to hemicellulose and cellulose decomposition respectively, and a smaller weight loss around 400 ºC (3), associated with lignin degradation (see Fig. 1). This data is consistent with the one obtained in a previous study carried out by our research group [10]. As expected from CSS TGA (see Fig. 1), pyrolysis at 280 ºC resulted in the degradation of hemicellulose. This was reflected in 280 ºC CSS biochar TGA, where only cellulose (2) and lignin (3) decomposition peaks were observed. In the same way, pyrolysis at 400 ºC degraded hemicellulose and cellulose, resulting in a lignin-based biochar. Lignin decomposition peaks (3) shown in Fig. 1-B were very low due to the low lignin content of CSS (1% wt.) [34]. It is also shown that lignin from CSS and 280 ºC CSS biochar degraded at around 250 ºC to 500 ºC, presenting small and wide peaks with a maximum at 400 ºC; however, in 400 ºC CSS biochar, part of lignin had already degraded and the peak (3) narrowed from 400 ºC to 500 ºC, changing its maximum to 470 ºC. This could be due to structural modifications of lignin at elevated temperatures [14]. Concerning the pyrolysis at 500 ºC, all three polymers were decomposed since 500 °C corresponded to approximately the end of CSS biomass thermal degradation; this is evidenced in CSS and 500 ºC CSS biochar TGA (see Fig. 1). As the resulting CSS biochars presented different hemicellulose, cellulose and lignin compositions, they are expected to have distinct properties from each other, which would be reflected in different potential applications.

3.1.2 Product yields

Slow pyrolysis of CSS, at 280 °C, 400 °C and 500 °C, resulted in the yields shown in Table 1, information that contributes to determine the best CSS pyrolysis temperature in function of the desired products.

Table 1

Product yields from the slow pyrolysis of CSS at the following temperatures. Data is expressed as wt. % on dry feedstock basis. (T, temperature; AP, aqueous phase of the pyrolysis liquid; NAP, non-aqueous phase of the pyrolysis liquid)

T (ºC)	Solid (wt. %)	Liquid		Gas (wt. %)	Losses (wt. %)
		AP (wt. %)	NAP (wt. %)		
280	80.5	4.1	-	10.3	5.1
400	40.5	15.4	18.2	20.7	5.2
500	31.5	15.7	22.5	22.4	7.9

Product distribution trends of CSS, shown in Table 1, are in accordance with the common thermal degradation of biomass: biochar yield (%solid) decreased with temperature, while liquid (%AP, %NAP) and gas fractions increased. Biochar yields were also consistent with CSS TGA, that showed 80.7%, 43.6% and 33.7% of solid weight at 280 ºC, 400 ºC and 500 ºC, respectively (see Table 1 and Fig. 1). The slight differences between TGA data and biochar yields are mainly related to the differences between heat transfer of the processes. Regarding the liquid fraction, and based on TGA data (Section 3.1.1), the aqueous phase (AP) was mainly composed of the hydrophilic products from hemicellulose decomposition in the 280 ºC case, and hemicellulose and cellulose degradation in the 400 ºC and 500 ºC pyrolysis liquids. On the other hand, non-aqueous phase (NAP) mainly consisted of hydrophobic products from partial (400 ºC) and total (500 ºC) decomposition of lignin [10]. According to the hydrophilicity and hydrophobicity of pyrolysis liquid compounds, they usually separate in two phases, AP and NAP, as in the present case [9,35]. The pyrolysis process resulted in a mass loss of about 5.0 - 7.9% (see Table 1), which is mainly associated

with the fact that some solid pyrolysis products could have remained inside the reactor. The obtained losses values are nevertheless acceptable for the scale of the reactor.

3.2 Feedstock and biochars

3.2.1 Solid product characterisation

Raw CSS and biochars from the slow pyrolysis of CSS (see Fig. 2) were studied and characterised in order to determine their potential uses, paying particular attention to their role as adsorbents in aqueous media.

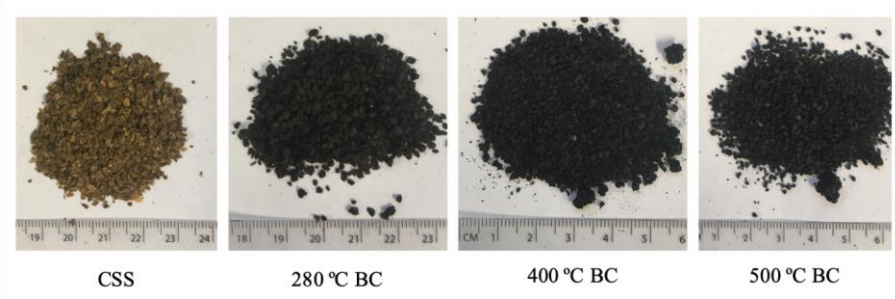

Fig. 2. CSS and biochars from the slow pyrolysis of CSS at 280 °C, 400 °C and 500 °C. The unit of the ruler is in cm. (CCS, coffee silverskin; BC, biochar)

Formatted: Font color: Text 1

Table 2

Characterization of CSS and biochars from the slow pyrolysis of CSS at 280 °C, 400 °C and 500 °C. Data is expressed as Mean **(**standard deviation). Ash, proximate and ultimate analysis are expressed as wt % on dry basis. (CCS, coffee silverskin; BC, biochar; VM, volatile matter; FC, fixed carbon; HHV, higher heating value; BET surface area)

	CSS	BC 280 ºC	BC 400 ºC	BC 500 ºC
Ash (% large oven)	8.34 (0.11)	8.01 (0.14)	16.51 (0.36)	21.81 (0.11)
Density (g/mL)	0.31 (0.01)	0.26 (0.00)	0.20 (0.00)	0.19 (0.01)

pH	5.35 (0.03)	6.66 (0.04)	8.9 (0.00)	10.05 (0.05)
Proximate Analysis				
VM (%)	76.41 (0.05)	70.43 (0.67)	41.80 (0.16)	38.53 (1.74)
FC (%) [1]	16.07 (0.18)	20.95 (1.22)	41.90 (0.37)	40.74 (0.66)
Ash (%)	7.52 (0.13)	8.62 (0.55)	16.29 (0.53)	20.72 (1.08)
Ultimate Analysis				
N (%)	3.50 (0.07)	3.37 (0.09)	3.10 (0.02)	2.90 (0.05)
C (%)	47.69 (0.02)	54.23 (0.39)	60.10 (0.61)	60.78 (0.72)
H (%)	5.61 (0.00)	5.87 (0.02)	4.44 (0.07)	2.59 (0.05)
S (%)	0.24 (0.02)	0.11 (0.01)	0.04 (0.06)	0.15 (0.02)
O (%) [1]	34.66 (0.02)	28.42 (0.49)	15.92 (0.62)	11.78 (0.84)
Molar H/C	1.40 (0.00)	1.29 (0.00)	0.88 (0.02)	0.51 (0.00)
Molar O/C	0.55 (0.00)	0.39 (0.01)	0.20 (0.01)	0.15 (0.01)
Molar (O+N)/C	0.61 (0.00)	0.45 (0.01)	0.24 (0.01)	0.19 (0.01)
HHV (MJ/kg) [2]	19.47 (0.01)	22.70 (0.21)	24.18 (0.21)	22.56 (0.39)
N_2 Porosimeter				
BET (m^2/g)	-	-	3.6	2.3
Pore size (nm)	-	-	39.6	88.8

[1] Fixed carbon and oxygen content are calculated by difference.

[2] HHV is calculated mathematically from Channiwala and Parikh [32] formula.

The analyses performed on CSS and CSS biochars are summarised in Table 2 and Fig. 3. Proximate analysis shows, as expected, a relative increase of ash content and fixed carbon with temperature, at the expense of volatile matter (see Table 2) [15]. This has also been observed in the previous section (3.1.1), where the number of volatile compounds removed from CSS increased with increasing the temperature of the pyrolysis process (see Fig. 1). In the same way, density decreased with increasing temperature due to the removal of volatile compounds. Ash data, which were obtained by different methods (oven and proximate analysis), presented similar results, with the highest difference between the values being 1%,

for the 500 ºC biochar (see Table 2). This biochar also presented the highest ash value (21%) as a result of the concentration of inorganic compounds with the temperature.

Regarding pH, it increased substantially at higher temperatures due to the increased relative concentration of basic surface oxides of alkali and alkaline earth metals [9] (see Table 2). The main metals present in the CSS are, specifically, potassium (27 mg/g), calcium (7 mg/g) and magnesium (3 mg/g) [10]. During pyrolysis, the mineral content of feedstock is largely retained and concentrated in biochars [37], justifying the basic pH of CSS biochars.

In reference to ultimate analysis, pyrolysis performed at high temperatures led to high degrees of carbonisation (see Table 2), that resulted in the formation of aromatic and graphitic structures on the biochar [31]. This fact is supported by increasing %C, and %H and %O decreasing, with increasing pyrolysis temperature. Molar ratios of the elements have been used to estimate the aromaticity (H:C), polarity (O:C) and oxygen functionality ((O+N):C) of chars [38], information that can be related to their behaviour as adsorbents. The reduction of these values indicates the removal of polar surface functional groups and the formation of aromatic structures through a higher degree of carbonization [31]. Specifically, the molar H/C ratio of ≤ 0.3 suggests highly condensed aromatic ring systems, and the lower molar O/C ratio, produced at higher temperature, indicated the arrangement of aromatic rings, originating stable crystal graphite-like structures [15]. In this way, with increasing temperature, biomass underwent dehydration and decarboxylation reactions, forming volatile dissociation products of lignin, cellulose and hemicelluloses, and condensation reactions, forming the graphitic structures [39,40]. Hence, as shown in Table 2, the more aromatic and less polar biochar was the one produced at 500 ºC. Ultimate analysis also suggests the potential use of CSS biochars as compost due to their high amount of nitrogen (>2%) compared to other composting materials, such as cow dung (1.87 %N) [41]. On the other hand, the carbon content of biochars, which was higher than 50% of the dry mass, complies

Field Code Changed

Formatted: Font color: Text 1

Field Code Changed

with the European Biochar Certificate (EBC) requirements [42]. This indicates that the biochars produced from CSS can be potentially used in soil applications, although limited by a relatively high ash content.

Calorific values (HHV) also indicates the use of CSS biochars for combustion purposes, as already observed in a previous study by our research group [10] (see Table 2). The heating values of biochars, with no significant differences between them, were similar to other fuels such as coal (14.6 – 26.7 kJ/kg) [43,44], representing an ideal alternative to renewable energy [11]. The increase of the biochar energy value compared to CSS feedstock is related to the increase of %C and the decrease of %O in biochars [40]. The low sulphur content of biochars (0.04-0.15 % wt.) can also favour their use as energy source due to the low sulphur oxides emissions that would be released in the combustion of biochars (see Table 2).

Concerning the role of CSS biochars as adsorbents, porosimetry and FTIR analysis, shown in Table 2 and Fig. 3., give information about properties associated to the adsorption capacity of biochars. Nitrogen porosimetry informs about the surface area (BET) and pore size distribution, which are related to the amount of active adsorption sites and the size of potential adsorbates, respectively. The analysis was carried out on the 400 ºC and 500 ºC biochars since appreciable surface area values are only expected for the highest pyrolysis temperatures [31]. This is because surface areas typically increase with increasing pyrolytic temperature due to the escape of volatile substances and the formation of channel/pore structures [45]. Nevertheless, the obtained surface areas were extremely low (< 4 m^2/g) (see Table 2). This fact can be explained due to the relatively low pyrolysis temperature, and the lack of an activation treatment, which are widely used to increase the surface area of biochars during the pyrolysis process [46]. Apart from that, porosity is also related to the lignin content of feedstock. Lignin-rich biomass, together with high pyrolysis temperature, typically results in high surface areas because of structural modifications of lignin at elevated

temperature, after the release of volatiles [14]. The role that lignin plays in porosimetry is not only as a precursor but also as a pore-size controller [47]. Hence, the low lignin content of CSS (1%, wt.) [34] contributed as well to the low porosity of biochars. Furthermore, biochar pores could be plugged by inorganic compounds from ash, tars (condensed volatiles), and other amorphous decomposition products which are known to partially block the micropores [14]. In this case, blocking of the pores could be favoured due to the relatively long vapour residence time in the reactor during the slow pyrolysis, putting the vapour in contact with the solid product for longer time.

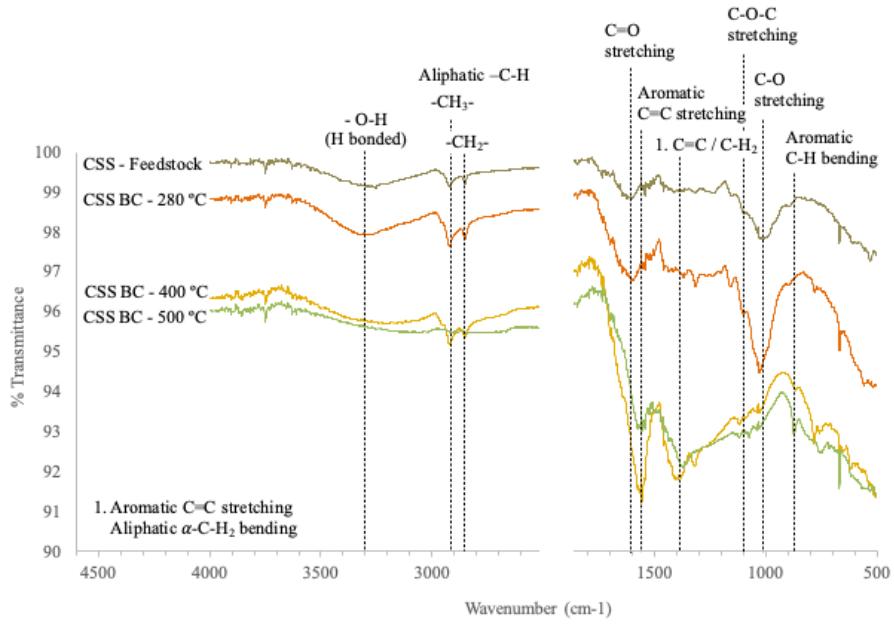

Fig. 3. FTIR spectra for CSS feedstock and CSS biochars. (CCS, coffee silverskin; BC, biochar)

FTIR, on the other hand, indicated the functional groups located on the surface of CSS feedstock and CSS biochars, which affects their potential interactions with adsorbates [15].

As observed in Fig. 3, and in agreement with the ultimate analysis from Table 2, polar functional groups were removed, and aromatic structures were formed with increasing pyrolysis temperature. A broad peak around 3300 cm^{-1}, corresponding to O-H stretching for alcohols and phenols, and a 2800-3000 cm^{-1} peak, attributable to aliphatic C-H stretching, were present in CSS, 280 ºC and 400 ºC biochars, but not in 500 ºC biochar [31,38]. Similar results were seen by Uchimiya et al. [31] in a study of cottonseed hulls biochars. Reduction of C=O (around 1600 cm^{-1}), related to carboxylate group, and C-O (1078 cm^{-1} for COC and 1000 cm^{-1} for acidic CO) were also observed in 400 ºC and 500 ºC biochars [30,31]. By contrast, aromatic peaks from C=C stretching (1566 cm^{-1}), as well as C–H bending (874 cm^{-1}) increased in 400 ºC and 500 ºC biochars [13,31,38]. The reduction of the polar functional groups, from dehydration and depolymerisation reactions during the pyrolysis process, led to the growth of aromatic and graphitic structures [38], which can interact with aromatic species. Hence, although the porosity of CSS biochars was low, their surface chemical characteristics indicated that they could be used as potential adsorbents of aromatic organic pollutants.

3.2.2 Adsorption of MB and MO from aqueous solution

This section is focused on studying the adsorbent properties of CSS biochars in aqueous media. This would demonstrate their potential use to remove contaminants from water, increasing the value of the biochar and promoting a CSS pyrolysis-based biorefinery by using the resulting solid, liquid and gas pyrolysis products for different purposes.

The study was carried out using MB and MO as model compounds (see Fig. 4) which allowed to evaluate the potential removal efficiency of aromatic ionic pollutants by CSS biochar.

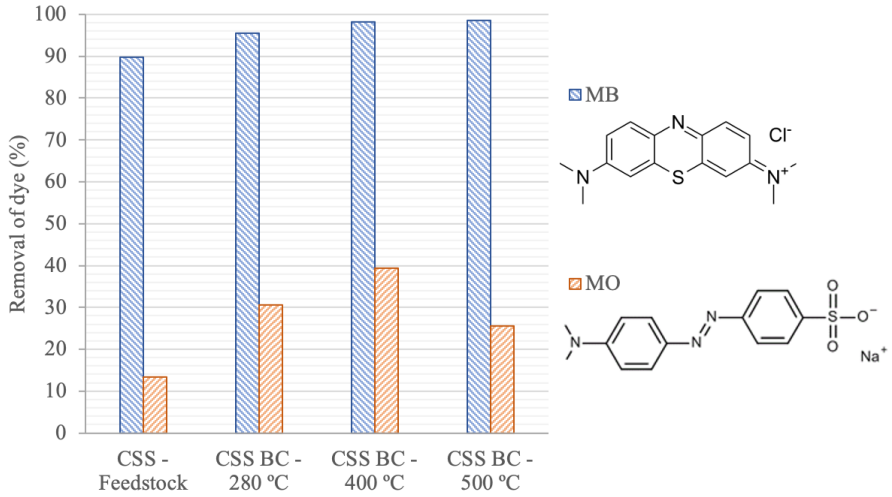

Fig. 4. Removal (%) of MB and MO from an aqueous solution with CSS feedstock and CSS biochars. (CCS, coffee silverskin; MB, methylene blue; MO, methyl orange; BC, biochar).

Formatted: Indent: Left: 0 cm

As shown in Fig. 4, CSS biochars were efficient in removing MB and, to a lesser extent, MO, with 400 ºC CSS biochar being the best one in both cases, reaching respectively 98% and 40% removal. CSS feedstock also showed high MB removal values; however, with the production of biochar, it is also obtained liquid and solid products, which could be used as chemical and energy sources respectively, making pyrolysis a potential treatment for CSS. The affinity of biochars with MB and MO can be explained by π– π dispersion interaction between the aromatic rings of dyes and the aromatic structure of biochars (see Section 3.2.1, ultimate analysis) [26,48]. The functional groups present on the biochar surface (see Section 3.2.1, FTIR analysis) can also play a major role in MB and MO adsorption, especially by means of electrostatic interactions, electron donor-acceptor and hydrogen bonding mechanisms [26]. Electrostatic interactions may take place between the negatively charged carboxylate of biochars and the charged groups of the dyes (See Fig. 4). In the MB case,

there can be an electrostatic attraction between the nitrogen positive charge of MB and the biochars [26], whereas concerning MO, there can be a repulsion force between the negatively-charged sulphonic group of MO and carboxylate anions of biochars, leading to lower levels of removal of MO compared to MB. The differences between MB and MO were reflected in Fig. 4, where MB removal values were substantially higher than the MO ones. Electron donor-acceptor interactions, on the other hand, could take place between carbonyl oxygens in the biochar, that would act as an electron donor, and the aromatic ring of MB and MO, that would be the electron acceptor [26]. In terms of hydrogen bonds, they could be formed between hydroxyl groups of biochars and nitrogen from MB and MO [26]. As CSS presents low lignin content [34], most of the hydroxyl groups originated from hemicellulose and cellulose. The restrictive effect of the hydrogen-bond network of cellulose molecules leads to hydroxyl groups having low accessibility on the biomass surface [19]. In this regard, the main contribution in MB and MO adsorption would be $\pi-\pi$ dispersion and electrostatic interactions.

Based on the MB and MO main mechanisms, CSS biochar could be used to remove compounds with aromatic rings in their structure from water, and especially compounds with positive charge. Examples of this could be aromatic antiepileptic drugs (AED), sulphonamides (synthetic bacteriostatic antibiotics), thiacloprid pesticide, estrogens, ibuprofen and paracetamol derivates, apart from the MB and MO dyes themselves [13,17,48]. Particularly in MB case, CSS biochars, which were performed without any activation treatment, presented similar removal values as a commercial activated carbon (Norit) (≥99% removal) shown in a previous work [49], with removal rates of 95.5% with 280 ºC biochar (38.1 mg MB/ g biochar), 98.2 % with 400 ºC biochar (39.3 mg MB/ g biochar) and 98.5 % with 500 ºC biochar (39.4 mg MB/ g biochar) (See Fig. 4). Commercial activated carbons are known to have the highest removal efficiency since their large surface area and presence

of surface functional groups facilitate interactions with various compounds [26]; however, their resource- and energy-intensive production process also makes them expensive products [13]. In this way, CSS biochars could be a potential sustainable and more affordable alternative to activated carbon for the adsorption of cationic aromatic compounds, as they present a similar structure to MB. Apart from organic pollutants, CSS biochars could be also effective in the removal of cationic heavy metals by means of electrostatic attraction [13] or complexation with carbonyl groups of biochar [16], considering that the contamination of water by toxic metals has become a pervasive problem throughout the world [13]. Biochars have also significant potential to address not just the pollutants in water, but also in soil and gaseous media [11].

Formatted: Font color: Text 1
Field Code Changed
Field Code Changed
Field Code Changed

3.3 Pyrolysis liquid

3.3.1 Pyrolysis liquid description

Slow pyrolysis of CSS at 280 °C, 400 °C and 500 °C also resulted in the pyrolysis liquid shown in Fig. 5. As shown, 280 ºC pyrolysis liquid consisted of a single aqueous phase; on the other hand, 400 ºC and 500 ºC pyrolysis liquids were composed of two phases, an aqueous phase and a non-aqueous phase. This is because this type of pyrolysis generates high amounts of reaction water, separating the hydrophilic and hydrophobic compounds of pyrolysis liquid in two phases [9,35]. As hydrophobic compounds are mainly from lignin degradation [9,33], the phase separation only took place at 400 ºC and 500 ºC, at which a higher amount of lignin has been decomposed (see Section 3.1.1). On the contrary, hydrophilic compounds are mostly from hemicellulose, cellulose and part of lignin decomposition [9,33,50].

Formatted: Font color: Text 1

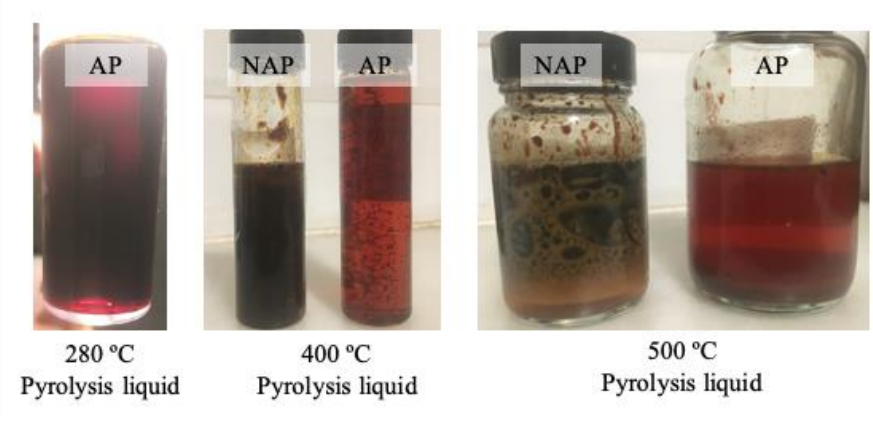

Fig. 5. Pyrolysis liquids from the slow pyrolysis of CSS at 280 °C, 400 °C and 500 °C. (CCS, coffee silverskin; AP, aqueous phase of the pyrolysis liquid; NAP, non-aqueous phase of the pyrolysis liquid)

3.3.2 Pyrolysis liquid composition

The chemical composition of the CSS pyrolysis liquids was analysed by GC-MS (see Fig. 6), showing caffeine as the most abundant compound in all samples. In contrast with pyrolysis liquid from classical forest biomass [51,52] or other agricultural wastes, such as grape pomace [33] or olive mill waste [9], CSS pyrolysis liquids showed low phenolic content. This is due to most of the phenolics originating from the degradation of lignin, which is low in CSS (1% wt.) [34]. It is also observed that CSS pyrolysis liquids were particularly rich in nitrogen compounds, since the amount of nitrogen present in CSS was high (3%) (see Section 3.2.1, ultimate analysis). This characteristic was detected as well by Polidoro et al. [8] and in the previous study performed by our research group [10].

As shown in Fig. 6, 400 ºC and 500 ºC pyrolysis liquids presented similar compositions, which were much higher than the one at 280 ºC, as expected from TGA data that showed lower devolatilisation at 280 ºC (see Section 3.1.1). AP (Graphic A) was mainly composed of

caffeine (compound 19) and to a lesser extent, pyridine (2), phenolics (13, 15, 16) and other low molecular weight oxygenated products (1, 5, 7, 8, 9, 11, 12). NAP (Graphic B), on the other hand, mostly contained caffeine (16), phenolics (5, 7, 8, 9, 10, 11), nitrogenated compounds (1, 2, 12, 13), hydrocarbon chains (14, 15, 17) and sterols (18, 19). Hence, CSS pyrolysis liquids seem to be a potential source of caffeine (see Fig. 6), which is a value-added compound widely used in food and pharmaceutical industry [27–29].

Table 3

Content of caffeine in aqueous phase of pyrolysis liquid from the slow pyrolysis of CSS at 280 ºC, 400 ºC and 500 ºC (CSS, Coffee Silverskin; AP, Aqueous Phase of the pyrolysis liquid).

Caffeine concentration	**AP 280 ºC**	**AP 400 ºC**	**AP 500 ºC**
In aqueous phase (g caffeine/L AP**)**	11.5	14.3	10.4
From feedstock (mg caffeine AP/g CSS**)**	1.75	3.81	2.81

In this regard, caffeine concentration from AP samples was quantified by HPLC-UV/Vis (see Table 3), with AP 400 ºC showing the highest amount of caffeine (14.3 g caffeine /L AP; 3.81 mg caffeine AP/ g CSS). Specifically, from each tonne of CSS, it was obtained 154 kg of AP (400 ºC), which contained 2 kg of caffeine. It is reported that the total content of caffeine in CSS feedstock is around 4.4 – 10.0 mg caffeine /g CSS by Bresciani et al. [53], 8.3 – 13.7 mg caffeine /g CSS by Napolitano et al. [54], and 7.7 – 10.3 mg caffeine /g CSS by Toschi et al. [55], the difference between these values being attributed to the different methods used for its measurement [55]. In view of this data, it is assumed that just part of

Formatted: Font color: Text 1, English (United Kingdom)
Formatted: Font color: Text 1
Formatted: Font color: Text 1
Formatted: Font color: Text 1

539 CSS caffeine was concentrated in the AP liquid fractions, while the rest should be in the NAP
540 pyrolysis liquids (see Fig 7, graphic B). Still, CSS AP pyrolysis liquids, mainly the 400 ºC
541 sample, contained an appreciable concentration of caffeine.

542 Apart from caffeine, CSS pyrolysis liquids were also composed of other value-added
543 products, such as phenolics and β-sitosterol (19, Fig. 6.B). Phenolics are known for their
544 antioxidant properties, which are highly valuated in nutraceuticals and cosmetic industries
545 [9,10]. Specifically, our previous study determined the total phenolic content and the
546 antioxidant capacity of 280 ºC, 400 ºC and 500 ºC CSS pyrolysis liquids, showing them as
547 potential source of phenolics [10]. On the other hand, β-sitosterol is usually used in medicine
548 for heart disease, hypercholesterolemia, modulating the immune system, prevention of
549 cancer, as well as for rheumatoid arthritis, tuberculosis, cervical cancer, hair loss and benign
550 prostatic hyperplasia [56]. In this way, CSS pyrolysis liquids could be considered as potential
551 sources of value-added products, in particular caffeine, which amount between 10.4 and 14.3
552 g/L in the AP. It should be noted that these products need to be first separated and purified.

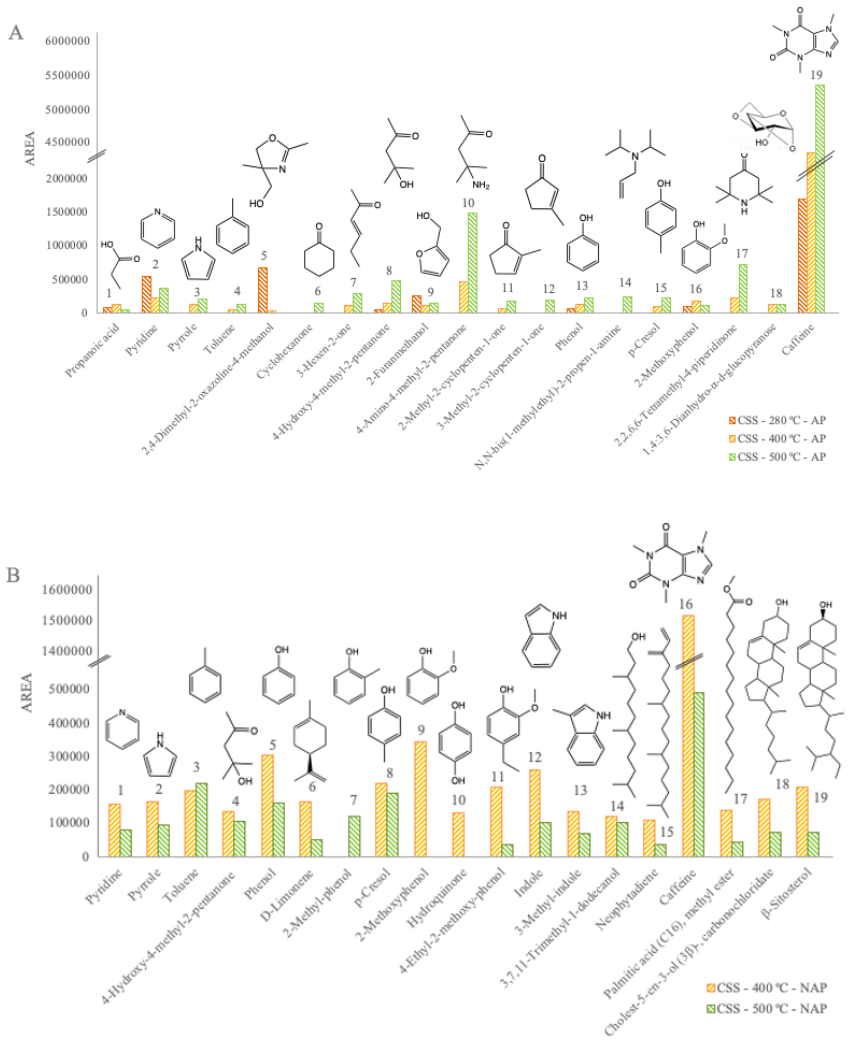

Fig. 6. Most abundant compounds of AP (A) and NAP (B) phases of CSS pyrolysis liquids determined by GC-MS analysis. (CCS, coffee silverskin; AP, aqueous phase of the pyrolysis liquid; NAP, non-aqueous phase of the pyrolysis liquid)

3.4 Gas fraction

559 CSS pyrolysis gases mainly consisted of CO_2, CO, CH_4, and, to a lesser extent, H_2, C_2H_6,
560 C_2H_4 and C_3H_8 (see Table 4). From all gases, CO_2 was the most abundant compound,
561 followed by CO. CO_2 and CO are related to the pyrolysis of hemicellulose and cellulose [57],
562 the first polymers to be thermally degraded (see Section 3.1.1). CO_2 is mainly released from
563 the cracking and reforming of carboxyl (C=O) and carboxylic acid (COOH), mostly present
564 in hemicellulose, whereas CO is mainly obtained from carbonyl (COC) and carboxyl (C=O)
565 decomposition, mostly concentrated in cellulose [57]. On the contrary, H_2 gave low
566 percentages, being almost negligible at low pyrolysis temperatures (see Table 4). Similar
567 results were obtained by Yu et al. [30] in the pyrolysis of rice husk and corn stalk, performed
568 in the same auger reactor as the present study, where H_2 percentage was not significant till
569 pyrolysis temperatures were above 500 - 550 ºC [30,57]. Regarding CH_4 and the other light
570 hydrocarbons, they are attributed to the reforming and cracking of methoxyl groups, mainly
571 present in lignin, and heavier hydrocarbons [30,57].

572 Moreover, Table 4 shows that as the temperature of the pyrolysis process was increased, the
573 proportion of CO_2 decreased, and the proportions of the other gas compounds increased, as
574 also observed by Yu et al. [30]. This fact is reflected in the gas calorific values, which
575 increased with the increase in CH_4 and light hydrocarbons [58]. In this way, 500 ºC gas gave
576 the highest calorific value (10.25 MJ/m^3). The heat of combustion of the pyrolysis gases
577 could be used for biomass drying before thermochemical treatment, since the feedstock
578 should have low moisture content (typically no more than 10 wt. % of moisture).
579 Specifically, the resulting flue gas could be used as a drying medium in a direct rotary drums
580 and belt conventional dryers, where biomass could be heated by the hot flue gas directly
581 using the thermal energy in the hot gas [59]. Hence, the integration of biomass drying to
582 pyrolysis process could improve the overall efficiency of the process, apart from contributing
583 to the circular economy and the bioeconomy.

Table 4

HHVs and composition of gas fractions from the slow pyrolysis of CSS at 280 ºC, 400 ºC and 500 ºC. Data of gas composition is expressed as % vol, obtained from GC analysis. (HHV, higher heating value; CCS, coffee silverskin)

	Gas fraction		
	280 ºC	**400 ºC**	**500 ºC**
HHV (MJ/m^3)	1.88	3.79	10.25
Gas composition (%vol)			
CO_2	84.21	74.48	54.42
CO	15.44	23.07	26.23
CH_4	0.07	1.41	9.47
H_2	0.21	0.18	5.16
C_2H_6	0.02	0.45	2.98
C_2H_4	0.05	0.25	0.97
C_3H_8	0.00	0.16	0.77

4. Conclusions

The present work deals with the management of CSS, which is the only by-product from the coffee roasting process. By employing slow pyrolysis, it allows closer biorefinery integration of CSS by exploring the potential uses of the resulting fractions, demonstrating biochar as an adsorbent of mainly cationic and aromatic organic pollutants from water; pyrolysis liquid as caffeine source; and gas fraction as a heat source for biomass drying before pyrolysis treatments. Specifically, pyrolysis of one tonne of CSS at 400 ºC would generate 405 kg of biochar and could result in up to 2 kg of caffeine to be extracted from the aqueous pyrolysis

liquid fraction. This study promotes the sustainability, circular economy and zero-waste in the coffee roasting industry.

Declaration of competing interest

The authors declare that they have no known competing financial interest or personal relationships that could have appeared to influence the work reported in this paper

Acknowledgements

C. del Pozo expresses her gratitude to the Universitat Autònoma de Barcelona for funding her PhD contract through a PIF grant, as well as an Erasmus+ grant to support her exchange stay at Aston University (EBRI).

References

[1] R.C. Alves, F. Rodrigues, M. Antónia Nunes, A.F. Vinha, M.B.P.P. Oliveira, State of the art in coffee processing by-products, Elsevier Inc., 2017. https://doi.org/10.1016/B978-0-12-811290-8.00001-3.

[2] R.C. Borrelli, F. Esposito, A. Napolitano, A. Ritieni, V. Fogliano, Characterization of a New Potential Functional Ingredient: Coffee Silverskin, J. Agric. Food Chem. 52 (2004) 1338–1343. https://doi.org/10.1021/jf034974x.

[3] The Coffee Guide, (n.d.). http://www.thecoffeeguide.org/coffee-guide/world-coffee-trade/conversions-and-statistics/ (accessed August 27, 2020).

[4] Y. Narita, I. Kuniyo, Review on utilization and composition of coffee silverskin, Food Res. Int. 61 (2014) 16–22. https://doi.org/http://dx.doi.org/10.1016/j.foodres.2014.01.023.

[5] International Coffee Organization, World coffee consumption, (2020). http://www.ico.org/prices/new-consumption-table.pdf (accessed March 15, 2020).

[6] S.M.F. Bessada, R.C. Alves, M.B.P.P. Oliveira, Coffee silverskin: A review on potential cosmetic applications, Cosmetics. 5 (2018). https://doi.org/10.3390/cosmetics5010005.

[7] A.S.G. Costa, R.C. Alves, A.F. Vinha, S.V.P. Barreira, M.A. Nunes, L.M. Cunha, M.B.P.P. Oliveira, Optimization of antioxidants extraction from coffee silverskin, a roasting by-product, having in view a sustainable process, Ind. Crops Prod. 53 (2014) 350–357. https://doi.org/10.1016/j.indcrop.2014.01.006.

[8] A. dos S. Polidoro, E. Scapin, E. Lazzari, A.N. Silva, A.L. dos Santos, E.B. Caramao, R.A. Jacques, Valorization of coffee silverskin industrial waste by pyrolysis : From optimization of bio-oil production to chemical characterization by GC × GC / qMS, J. Anal. Appl. Pyrolysis. 129 (2018) 43–52. https://doi.org/10.1016/j.jaap.2017.12.005.

[9] C. del Pozo, J. Bartrolí, N. Puy, E. Fàbregas, Separation of value-added chemical groups from bio-oil of olive mill waste, Ind. Crops Prod. 125 (2018). https://doi.org/10.1016/j.indcrop.2018.08.062.

[10] C. del Pozo, J. Bartrolí, S. Alier, N. Puy, E. Fàbregas, Production of antioxidants and other value-added compounds from coffee silverskin via pyrolysis under a biorefinery approach, Waste Manag. 109 (2020) 19–27. https://doi.org/10.1016/j.wasman.2020.04.044.

[11] Y. Dai, N. Zhang, C. Xing, Q. Cui, Q. Sun, The adsorption, regeneration and engineering applications of biochar for removal organic pollutants: A review, Chemosphere. 223 (2019) 12–27. https://doi.org/10.1016/j.chemosphere.2019.01.161.

[12] T. Chen, R. Liu, N.R. Scott, Characterization of energy carriers obtained from the

pyrolysis of white ash, switchgrass and corn stover - Biochar, syngas and bio-oil, Fuel Process. Technol. 142 (2016) 124–134. https://doi.org/10.1016/j.fuproc.2015.09.034.

[13] X. Tan, Y. Liu, G. Zeng, X. Wang, X. Hu, Y. Gu, Z. Yang, Application of biochar for the removal of pollutants from aqueous solutions, Chemosphere. 125 (2015) 70–85. https://doi.org/10.1016/j.chemosphere.2014.12.058.

[14] D. Rehrah, M.R. Reddy, J.M. Novak, R.R. Bansode, K.A. Schimmel, J. Yu, D.W. Watts, M. Ahmedna, Production and characterization of biochars from agricultural by-products for use in soil quality enhancement, J. Anal. Appl. Pyrolysis. 108 (2014) 301–309. https://doi.org/10.1016/j.jaap.2014.03.008.

[15] Y. Wang, R. Liu, Comparison of characteristics of twenty-one types of biochar and their ability to remove multi-heavy metals and methylene blue in solution, Fuel Process. Technol. 160 (2017) 55–63. https://doi.org/10.1016/j.fuproc.2017.02.019.

[16] Y. Wang, R. Liu, H2O2 treatment enhanced the heavy metals removal by manure biochar in aqueous solutions, Sci. Total Environ. 628–629 (2018) 1139–1148. https://doi.org/10.1016/j.scitotenv.2018.02.137.

[17] P. Zhang, H. Sun, L. Min, C. Ren, Biochars change the sorption and degradation of thiacloprid in soil: Insights into chemical and biological mechanisms, Environ. Pollut. 236 (2018) 158–167. https://doi.org/10.1016/j.envpol.2018.01.030.

[18] A. Jiang, Z. Cheng, Z. Shen, W. Guo, QSAR study on the removal efficiency of organic pollutants in supercritical water based on degradation temperature, Chem. Cent. J. 12 (2018) 1–8. https://doi.org/10.1186/s13065-018-0380-y.

[19] Y. Zhu, B. Yi, Q. Yuan, Y. Wu, M. Wang, S. Yan, Removal of methylene blue from aqueous solution by cattle manure-derived low temperature biochar, RSC Adv. 8 (2018) 19917–19929. https://doi.org/10.1039/c8ra03018a.

[20] J. Yu, X. Zhang, D. Wang, P. Li, Adsorption of methyl orange dye onto biochar adsorbent prepared from chicken manure, Water Sci. Technol. 77 (2018) 1303–1312. https://doi.org/10.2166/wst.2018.003.

[21] Y. Song, Y. Bian, F. Wang, M. Xu, N. Ni, X. Yang, C. Gu, X. Jiang, Dynamic Effects of Biochar on the Bacterial Community Structure in Soil Contaminated with Polycyclic Aromatic Hydrocarbons, J. Agric. Food Chem. 65 (2017) 6789–6796. https://doi.org/10.1021/acs.jafc.7b02887.

[22] A. Zhelezova, H. Cederlund, J. Stenström, Effect of Biochar Amendment and Ageing on Adsorption and Degradation of Two Herbicides, Water. Air. Soil Pollut. 228 (2017). https://doi.org/10.1007/s11270-017-3392-7.

[23] H. Liu, Y. Wei, J. Luo, T. Li, D. Wang, S. Luo, J.C. Crittenden, 3D hierarchical porous-structured biochar aerogel for rapid and efficient phenicol antibiotics removal from water, Chem. Eng. J. 368 (2019) 639–648. https://doi.org/10.1016/j.cej.2019.03.007.

[24] L. Li, M. Yang, Q. Lu, W. Zhu, H. Ma, L. Dai, Oxygen-rich biochar from torrefaction: A versatile adsorbent for water pollution control, Bioresour. Technol. 294 (2019) 122142. https://doi.org/10.1016/j.biortech.2019.122142.

[25] B.H. Hameed, A.T.M. Din, A.L. Ahmad, Adsorption of methylene blue onto bamboo-based activated carbon: Kinetics and equilibrium studies, J. Hazard. Mater. 141 (2007) 819–825. https://doi.org/10.1016/j.jhazmat.2006.07.049.

[26] A.M.M. Vargas, A.L. Cazetta, M.H. Kunita, T.L. Silva, V.C. Almeida, Adsorption of methylene blue on activated carbon produced from flamboyant pods (Delonix regia): Study of adsorption isotherms and kinetic models, Chem. Eng. J. 168 (2011) 722–730. https://doi.org/10.1016/j.cej.2011.01.067.

694 [27] A.F.M. Cláudio, A.M. Ferreira, M.G. Freire, J.A.P. Coutinho, Enhanced extraction of
695 caffeine from guaraná seeds using aqueous solutions of ionic liquids, Green Chem. 15
696 (2013) 2002–2010. https://doi.org/10.1039/c3gc40437d.
697 [28] A. Rahimi, M.A. Zanjanchi, S. Bakhtiari, M. Dehsaraei, Selective determination of
698 caffeine in foods with 3D-graphene based ultrasound-assisted magnetic solid phase
699 extraction, Food Chem. 262 (2018) 206–214.
700 https://doi.org/10.1016/j.foodchem.2018.04.035.
701 [29] C. Cai, F. Li, L. Liu, Z. Tan, Deep eutectic solvents used as the green media for the
702 efficient extraction of caffeine from Chinese dark tea, Sep. Purif. Technol. 227 (2019)
703 115723. https://doi.org/10.1016/j.seppur.2019.115723.
704 [30] Y. Yu, Y. Yang, Z. Cheng, P.H. Blanco, R. Liu, A. V. Bridgwater, J. Cai, Pyrolysis of
705 Rice Husk and Corn Stalk in Auger Reactor. 1. Characterization of Char and Gas at
706 Various Temperatures, Energy and Fuels. 30 (2016) 10568–10574.
707 https://doi.org/10.1021/acs.energyfuels.6b02276.
708 [31] M. Uchimiya, L.H. Wartelle, K.T. Klasson, C.A. Fortier, I.M. Lima, Influence of
709 pyrolysis temperature on biochar property and function as a heavy metal sorbent in
710 soil, J. Agric. Food Chem. 59 (2011) 2501–2510. https://doi.org/10.1021/jf104206c.
711 [32] S.A. Channiwala, P.P. Parikh, A unified correlation for estimating HHV of solid,
712 liquid and gaseous fuels, Fuel. 81 (2002) 1051–1063. https://doi.org/10.1016/S0016-
713 2361(01)00131-4.
714 [33] C. del Pozo, J. Bartrolí, S. Alier, N. Puy, E. Fàbregas, Production , identification , and
715 quantification of antioxidants from torrefaction and pyrolysis of grape pomace, Fuel
716 Process. Technol. 211 (2021) 106602. https://doi.org/10.1016/j.fuproc.2020.106602.
717 [34] P.S. Murthy, M. Madhava Naidu, Sustainable management of coffee industry by-

718 products and value addition - A review, Resour. Conserv. Recycl. 66 (2012) 45–58.
719 https://doi.org/10.1016/j.resconrec.2012.06.005.
720 [35] C. Torri, D. Fabbri, Biochar enables anaerobic digestion of aqueous phase from
721 intermediate pyrolysis of biomass, Bioresour. Technol. 172 (2014) 335–341.
722 https://doi.org/10.1016/j.biortech.2014.09.021.
723 [36] J.M. Novak, I.M. Lima, B. Xing, J.W. Gaskin, C. Steiner, K.C. Das, M. Ahmedna, D.
724 Rehrah, D.W. Watts, W.J. Busscher, H. Schomberg, Characterization of designer
725 biochar produced at different temperatures and their effects on a loamy sand, Ann.
726 Environ. Sci. 5 (2009) 195–206.
727 [37] K. Raveendran, A. Ganesh, K. Khilar, Influence of mineral matter on biomass
728 pyrolysis characteristic, Fuel. 74 (1995) 1812–1822.
729 [38] K. Lou, A.U. Rajapaksha, Y.S. Ok, S.X. Chang, Pyrolysis temperature and steam
730 activation effects on sorption of phosphate on pine sawdust biochars in aqueous
731 solutions, Chem. Speciat. Bioavailab. 28 (2016) 42–50.
732 https://doi.org/10.1080/09542299.2016.1165080.
733 [39] M. Keiluweit, P.S. Nico, M.G. Johnson, M. KLEBER, Dynamic Molecular Structure
734 of Plant Biomass-derived Black Carbon(Biochar)- Supporting Information -, Environ.
735 Sci. Technol. 44 (2010) 1247–1253. 10.1021/es9031419.
736 [40] Z. Liu, G. Han, Production of solid fuel biochar from waste biomass by low
737 temperature pyrolysis, FUEL. 158 (2015) 159–165.
738 https://doi.org/10.1016/j.fuel.2015.05.032.
739 [41] D.C. Preethu, B.N.U.H.B. Prakash, C.A. Srinivasamurthy, B.G. Vasanthi, Maturity
740 Indices as an Index to Evaluate the Quality of Compost of Coffee Waste Blended with
741 Other Organic Wastes, Proc. Int. Confer- Ence Sustain. Solid Waste Manag. Sept. 5–7,

Chennai, India,. (2007) 270–275.

[42] EBC (2012), European Biochar Certificate - Guidelines for a Sustainable Production of Biochar', Eur. Biochar Found. (EBC), Arbaz, Switzerland. Version 6.1 19th June,. (2015) 1–22. https://doi.org/10.13140/RG.2.1.4658.7043.

[43] M. Inguanzo, A. Domínguez, J.A. Menéndez, C.G. Blanco, J.J. Pis, On the pyrolysis of sewage sludge: The influence of pyrolysis temperature on biochar, liquid and gas fractions, J. Anal. Appl. Pyrolysis. 63 (2002) 209–222. https://doi.org/10.4028/www.scientific.net/AMR.518-523.3412.

[44] M.E. Sánchez, E. Lindao, D. Margaleff, O. Martínez, A. Morán, Pyrolysis of agricultural residues from rape and sunflowers: Production and characterization of bio-fuels and biochar soil management, J. Anal. Appl. Pyrolysis. 85 (2009) 142–144. https://doi.org/10.1016/j.jaap.2008.11.001.

[45] M. Ahmad, S.S. Lee, X. Dou, D. Mohan, J.K. Sung, J.E. Yang, Y.S. Ok, Effects of pyrolysis temperature on soybean stover- and peanut shell-derived biochar properties and TCE adsorption in water, Bioresour. Technol. 118 (2012) 536–544. https://doi.org/10.1016/j.biortech.2012.05.042.

[46] A.U. Rajapaksha, M. Vithanage, M. Zhang, M. Ahmad, D. Mohan, S.X. Chang, Y.S. Ok, Pyrolysis condition affected sulfamethazine sorption by tea waste biochars, Bioresour. Technol. 166 (2014) 303–308. https://doi.org/10.1016/j.biortech.2014.05.029.

[47] Z.K. Huang, Q.F. Lü, Q. Lin, X. Cheng, Microstructure, Properties and Lignin-Based Modification of Wood-Ceramics from Rice Husk and Coal Tar Pitch, J. Inorg. Organomet. Polym. Mater. 22 (2012) 1113–1121. https://doi.org/10.1007/s10904-012-9708-6.

766 [48] H.N. Tran, F. Tomul, N. Thi Hoang Ha, D.T. Nguyen, E.C. Lima, G.T. Le, C.T.
767 Chang, V. Masindi, S.H. Woo, Innovative spherical biochar for pharmaceutical
768 removal from water: Insight into adsorption mechanism, J. Hazard. Mater. 394 (2020)
769 122255. https://doi.org/10.1016/j.jhazmat.2020.122255.
770 [49] F. Rego, J. Wang, Y. Yang, A. V. Bridgwater, Development of an integrated and
771 continuous slow pyrolysis and activation process for the production of activated
772 carbon from waste biomass, Eur. Biomass Conf. Exhib. Proc. (2019) 1076–1079.
773 [50] J.P. Diebold, A Review of the chemical and physical mechanisms of the storage
774 stability of fast pyrolysis bio-oils, in: A.V. Bridgwater (Ed.), Fast Pyrolysis Biomass A
775 Handb., CPL Press, Newbury, UK, 2002: p. 424. https://doi.org/NREL/SR-570-27613.
776 [51] N. Puy, R. Murillo, M. V. Navarro, J.M. López, J. Rieradevall, G. Fowler, I.
777 Aranguren, T. García, J. Bartrolí, A.M. Mastral, Valorisation of forestry waste by
778 pyrolysis in an auger reactor, Waste Manag. 31 (2011) 1339–1349.
779 https://doi.org/10.1016/j.wasman.2011.01.020.
780 [52] A. Artigues, N. Puy, J. Bartrolí, E. Fábregas, Comparative Assessment of Internal
781 Standards for Quantitative Analysis of Bio-oil Compounds by Gas Chromatography /
782 Mass Spectrometry Using Statistical Criteria, Energy Fuels. 28 (2014) 3908–3915.
783 https://doi.org/10.1021/ef5005545.
784 [53] L. Bresciani, L. Calani, R. Bruni, F. Brighenti, D. Del Rio, Phenolic composition,
785 caffeine content and antioxidant capacity of coffee silverskin, Food Res. Int. 61 (2014)
786 196–201. https://doi.org/10.1016/j.foodres.2013.10.047.
787 [54] A. Napolitano, V. Fogliano, A. Tafuri, A. Ritieni, Natural occurrence of ochratoxin A
788 and antioxidant activities of green and roasted coffees and corresponding byproducts,
789 J. Agric. Food Chem. 55 (2007) 10499–10504. https://doi.org/10.1021/jf071959+.

[55] T.G. Toschi, V. Cardenia, G. Bonaga, M. Mandrioli, M.T. Rodriguez-Estrada, Coffee silverskin: Characterization, possible uses, and safety aspects, J. Agric. Food Chem. 62 (2014) 10836–10844. https://doi.org/10.1021/jf503200z.

[56] S. Saeidnia, A. Manayi, A.R. Gohari, M. Abdollahi, The Story of Beta-sitosterol- A Review, European J. Med. Plants. 4 (2014) 590–609. https://doi.org/10.9734/ejmp/2014/7764.

[57] T. Qu, W. Guo, L. Shen, J. Xiao, K. Zhao, Experimental Study of Biomass Pyrolysis Based on Three Major Components: Hemicellulose, Cellulose, and Lignin, Ind. Eng. Chem. Res. 50 (2011) 10424–10433. https://doi.org/dx.doi.org/10.1021/ie1025453.

[58] A. V. Bridgwater, Renewable fuels and chemicals by thermal processing of biomass, Chem. Eng. J. 91 (2003) 87–102. https://doi.org/10.1016/S1385-8947(02)00142-0.

[59] J. Yi, X. Li, J. He, X. Duan, Drying efficiency and product quality of biomass drying: a review, Dry. Technol. 0 (2019) 1–16. https://doi.org/10.1080/07373937.2019.1628772.